

## On the acoustic–electromagnetic analogy

José M. Carcione \*, Fabio Cavallini

*Osservatorio Geofisico Sperimentale, P.O. Box 2011 Opicina, I-34016 Trieste, Italy*

Received 1 June 1994; revised 2 November 1994

---

### Abstract

We investigate the analogy between electromagnetic and acoustic waves, considering the kinematics and the energy balance of wave propagation. It is shown that the propagation of the TEM mode (transverse electric and magnetic) is completely analogous, from the mathematical point of view, to the propagation of viscoelastic SH waves in the plane of symmetry of a monoclinic medium. The viscoelastic model corresponding to the electromagnetic equations is the 3D Maxwell constitutive law. The analogy identifies particle velocity with magnetic field, stresses with electric field, compliance with permittivity, inverse of the viscosity with conductivity, and density with permeability. Therefore, it is possible to compute simultaneously the phase velocity, the slowness, the attenuation, the quality factor and the energy velocity of both wave phenomena. The dissipation effects due to anisotropic viscosity and conductivity are verified by numerical experiments performed with spectral time-domain techniques, which have been chosen because accuracy is very important when there are physical dispersion and anisotropic dissipation. An analytical solution is found for elastic anisotropic media, and extended to the viscoelastic and electromagnetic cases by using the correspondence principle. Finally, two corresponding examples are worked out numerically, and an electromagnetic problem is solved with a computer code originally designed for solving viscoelastic wave propagation.

---

### 1. Introduction

Electromagnetic waves have been used by a wide variety of probing techniques designed to study the electrical properties of the earth. It is well known that the conductivity strongly depends on the rock characteristics such as pore geometry, clay content and water conductivity. In particular, in coal mining it is of interest to locate areas of geological disturbance such as sand channels or faults (e.g., Ref. [1]). On the other hand, acoustic waves are the main tool in geophysical prospecting of hydrocarbons. The seismic method is based on the reflection of acoustic waves from inhomogeneities and interfaces separating the geological formations.

As early as the 17th century it was known that light and acoustic waves are of similar nature. Hooke believed light to be a vibratory displacement of a medium, through which it propagates at finite speed. Later, in the 19th century, Maxwell and Lord Kelvin made extensive use of physical and mathematical analogies to study wave phenomena in acoustics and electromagnetism [2]. In fact, the displacement current term introduced by Maxwell into the electromagnetic equations arises from the analogy with elastic displacements. It is possible to recast the viscoelastodynamic equations into a form that closely parallels Maxwell's equation. In many cases, this formal analogy becomes a complete mathematical equivalence such that the problems in both fields can be solved by using the same analytical (or numerical) methodology.

---

\* Corresponding author.

In this work, it is shown that the 2D Maxwell equations describing propagation of the TEM mode in anisotropic media is completely analogous to the SH wave equation in a Maxwell anisotropic-viscoelastic solid. This equivalence was probably known to Maxwell, who was aware of the analogy between the process of conduction (static induction through dielectrics) and viscosity (elasticity). Actually, Maxwell's electromagnetic theory of light, including the conduction and displacement currents, was already completed in his paper "On physical lines of force" published in two parts in 1861 and 1862 [3]. On the other hand, the viscoelastic model was proposed in 1867 (see Refs. [4] and [5]). He seems to have arrived to the viscoelastic rheology from a comparison with Thomson's telegraphy equations (e.g., Ref. [6]), which describe the process of conduction and dissipation of electric energy through cables [2].

The analogy can be exploited in several ways. In first place, existing viscoelastodynamic modeling codes can be easily modified to simulate electromagnetic wave propagation. Secondly, the set of solutions of the viscoelastic SH problem, obtained from the correspondence principle, can be used to test the electromagnetic codes. Moreover, the theory of propagation of plane harmonic waves in anisotropic-viscoelastic media applies also to electromagnetic anisotropic wave propagation. In particular, the introduction of anisotropic effects is relevant in the study of sedimentary formations in which oil and gas are stored. Indeed, it is well known that velocity and attenuation anisotropy of acoustic waves are important in cracked limestones and thin saturated sandstones layers embedded in anisotropic shales. Moreover, the value of the electrical conductivity has a wide range (it may vary from  $10^{-14}$  to  $10^6$  S/m) and may present a high coefficient of anisotropy. In some cases, like interbedded shales and sandstones, the longitudinal conductivity can be as far as nine times the transverse conductivity. In this sense, electromagnetic attenuation effects can be very important hydrocarbon indicators.

The paper is organized as follows. Sections 2 and 3 introduce the electromagnetic and acoustic equations. The analogy is established in Section 4, including the correspondence with electric circuits. The kinematic and energy quantities describing wave propagation are obtained in Section 5. Finally, in Section 6 we solve numerically the field equations and compare the re-

sults with the theoretical predictions. In addition, the numerical modeling algorithm is tested with the problem of anisotropic electromagnetic propagation.

## 2. Maxwell's equations

In 3D vector notation, the Maxwell equations are (e.g., Ref. [7])

$$\nabla \times \mathbf{E} = -\frac{\partial \mathbf{B}}{\partial t} + \mathbf{M}, \quad (1)$$

$$\nabla \times \mathbf{H} = \frac{\partial \mathbf{D}}{\partial t} + \mathbf{J}, \quad (2)$$

where  $\mathbf{E}$ ,  $\mathbf{B}$ ,  $\mathbf{H}$  and  $\mathbf{D}$  are the electric intensity, the magnetic flux density, the magnetic intensity and the electric flux density, respectively, and  $\mathbf{J}$  and  $\mathbf{M}$  are the electric and magnetic current densities, respectively. In general, they depend on  $\mathbf{x} = (x, y, z)$ , the Cartesian coordinates, and  $t$ , the time variable. Equations (1) and (2) constitute six scalar equations with 12 scalar unknowns, since  $\mathbf{M}$  is assumed to be given and  $\mathbf{J}$  is a known function of the electric field as stated explicitly by Eq. (5) below. The six additional scalar equations are the constitutive relations, which for isotropic media can be written as

$$\mathbf{D} = \boldsymbol{\epsilon} \cdot \mathbf{E}, \quad (3)$$

$$\mathbf{B} = \boldsymbol{\mu} \cdot \mathbf{H}, \quad (4)$$

where  $\boldsymbol{\epsilon}$  and  $\boldsymbol{\mu}$  are the permittivity and permeability matrices, respectively. The dot in the r.h.s. of (3) and (4) denotes ordinary matrix multiplication. Moreover, the current density is

$$\mathbf{J} = \boldsymbol{\sigma} \cdot \mathbf{E} + \mathbf{J}_s, \quad (5)$$

where  $\boldsymbol{\sigma}$  is the conductivity matrix and  $\mathbf{J}_s$  is the given contribution of the sources, taken as zero in Section 4. The first term of the r.h.s. of (5) is the conduction current density. Substituting the constitutive relations and the current density into Eqs. (1) and (2) gives

$$\nabla \times \mathbf{E} = -\boldsymbol{\mu} \cdot \frac{\partial \mathbf{H}}{\partial t} + \mathbf{M}, \quad (6)$$

$$\nabla \times \mathbf{H} = \boldsymbol{\sigma} \cdot \mathbf{E} + \boldsymbol{\epsilon} \cdot \frac{\partial \mathbf{E}}{\partial t} + \mathbf{J}_s. \quad (7)$$

### 3. The acoustic field equations

The fundamental equations of acoustics, when written in terms of particle velocity and stress, can be expressed in terms of first order time derivatives. Following Auld [8], Cauchy's equations can be written as

$$\nabla \cdot \mathbf{T} = \rho \frac{\partial \mathbf{v}}{\partial t} - \mathbf{F}, \quad (8)$$

where

$$\mathbf{T} = [\sigma_{xx}, \sigma_{yy}, \sigma_{zz}, \sigma_{yz}, \sigma_{xz}, \sigma_{xy}]^T \quad (9)$$

is the stress vector,  $\mathbf{v}$  is the particle velocity vector,  $\rho$  is the density,  $\mathbf{F}$  is the body force vector, and, from now on,

$$\nabla = \begin{bmatrix} \partial/\partial x & 0 & 0 & 0 & \partial/\partial z & \partial/\partial y \\ 0 & \partial/\partial y & 0 & \partial/\partial z & 0 & \partial/\partial x \\ 0 & 0 & \partial/\partial z & \partial/\partial y & \partial/\partial x & 0 \end{bmatrix}. \quad (10)$$

The strain is given in terms of the displacement  $\mathbf{u} = [u_x, u_y, u_z]^T$  by

$$\mathbf{S} = [\epsilon_{xx}, \epsilon_{yy}, \epsilon_{zz}, 2\epsilon_{yz}, 2\epsilon_{xz}, 2\epsilon_{xy}]^T, \quad (11)$$

where  $\epsilon_{xx} = \partial u_x / \partial x$ ,  $\epsilon_{xy} = (\partial u_x / \partial y + \partial u_y / \partial x) / 2$ , etc. The relation between strain and particle velocity is

$$\nabla^T \cdot \mathbf{v} = \frac{\partial \mathbf{S}}{\partial t}. \quad (12)$$

Auld (see Ref. [8, p. 101]) establishes the acoustic–electromagnetic analogy by using a 3D Kelvin–Voigt model:

$$\mathbf{T} = \mathbf{c}_K \cdot \mathbf{S} + \boldsymbol{\eta}_K \cdot \frac{\partial \mathbf{S}}{\partial t}, \quad (13)$$

where  $\mathbf{c}_K$  and  $\boldsymbol{\eta}_K$  are the (Kelvin–Voigt) elasticity and viscosity matrices, respectively. Compare this relation to the 1D Kelvin–Voigt stress–strain relation in, e.g., Ref. [9, equation (10.43)]. Eliminating the time derivative of the strain by using Eq. (12), and defining the matrix

$$\boldsymbol{\tau}_K = \mathbf{c}_K^{-1} \cdot \boldsymbol{\eta}_K,$$

we get

$$\nabla^T \cdot \mathbf{v} + \boldsymbol{\tau}_K \cdot \nabla^T \frac{\partial \mathbf{v}}{\partial t} = \mathbf{c}_K^{-1} \cdot \frac{\partial \mathbf{T}}{\partial t}. \quad (14)$$

Auld establishes the analogy of (8) and (14) with Maxwell's equations (6) and (7), where  $\mathbf{T}$  corresponds to  $\mathbf{E}$  and  $\mathbf{v}$  corresponds to  $\mathbf{H}$ .

A better correspondence can be obtained by introducing, instead of (13), the 3D Maxwell constitutive relation [10]:

$$\frac{\partial \mathbf{S}}{\partial t} = \mathbf{c}_M^{-1} \cdot \frac{\partial \mathbf{T}}{\partial t} + \boldsymbol{\eta}_M^{-1} \cdot \mathbf{T}, \quad (15)$$

where  $\mathbf{c}_M$  and  $\boldsymbol{\eta}_M$  are the (Maxwell) elasticity and the viscosity matrices, respectively. Compare this relation to the 1D Maxwell stress–strain relation ([9, equation (10.34)]). Eliminating the strain, by using Eq. (12), gives the equation analogous to (7):

$$\nabla^T \cdot \mathbf{v} = \boldsymbol{\eta}_M^{-1} \cdot \mathbf{T} + \mathbf{c}_M^{-1} \cdot \frac{\partial \mathbf{T}}{\partial t}. \quad (16)$$

Defining the compliance matrix

$$\mathbf{s}_M = \mathbf{c}_M^{-1} \quad (17)$$

and the matrix

$$\boldsymbol{\tau}_M = \boldsymbol{\eta}_M^{-1}, \quad (18)$$

Eq. (16) becomes

$$\nabla^T \cdot \mathbf{v} = \boldsymbol{\tau}_M \cdot \mathbf{T} + \mathbf{s}_M \cdot \frac{\partial \mathbf{T}}{\partial t}. \quad (19)$$

In general, the analogy does not mean that acoustic and electromagnetic equations represent the same mathematical problem. In fact,  $\mathbf{T}$  is a 6D vector and  $\mathbf{E}$  is a 3D vector. Moreover, acoustics involves  $6 \times 6$  matrices (for material properties) and electromagnetism  $3 \times 3$  matrices. However, the complete equivalence can be established in the 2D case by using the Maxwell model, as can be seen in the next section.

### 4. Acoustic–electromagnetic analogy

In general, a realistic medium is described by symmetric anisotropic permittivity and conductivity tensors. Assume, for instance, that

$$\boldsymbol{\epsilon} = \begin{bmatrix} \epsilon_{11} & 0 & \epsilon_{13} \\ 0 & \epsilon_{22} & 0 \\ \epsilon_{13} & 0 & \epsilon_{33} \end{bmatrix} \quad (20)$$

and

$$\sigma = \begin{bmatrix} \sigma_{11} & 0 & \sigma_{13} \\ 0 & \sigma_{22} & 0 \\ \sigma_{13} & 0 & \sigma_{33} \end{bmatrix}. \quad (21)$$

Tensors (20) and (21) correspond to a monoclinic medium with the  $y$ -axis perpendicular to the plane of symmetry. There always exists a coordinate transformation that diagonalizes these symmetric matrices. This transformation is called the principal system of the medium, and gives the three principal components of these tensors. In cubic and isotropic media the principal components are all equal. In tetragonal and hexagonal materials two of the three parameters are equal. In orthorhombic, monoclinic, and triclinic media, all three components are unequal. The permeability tensor is, for most materials, isotropic. In this case, we have  $\mu = \mu \mathbf{1}$ ; here,  $\mu$  is the permeability and  $\mathbf{1}$  is the  $3 \times 3$  identity matrix.

Now, assume that the propagation is in the  $(x, z)$ -plane, and that the material properties are invariant in the  $y$ -direction. Then,  $E_x$ ,  $E_z$  and  $H_y$  are decoupled from  $E_y$ ,  $H_x$  and  $H_z$ . In the absence of electric source currents, the first three fields obey the TEM (transverse electric and magnetic fields) differential equations:

$$\frac{\partial E_z}{\partial x} - \frac{\partial E_x}{\partial z} = \mu \frac{\partial H_y}{\partial t} - M_y, \quad (22)$$

$$-\frac{\partial H_y}{\partial z} = \sigma_{11} E_x + \sigma_{13} E_z + \epsilon_{11} \frac{\partial E_x}{\partial t} + \epsilon_{13} \frac{\partial E_z}{\partial t}, \quad (23)$$

$$\frac{\partial H_y}{\partial x} = \sigma_{13} E_x + \sigma_{33} E_z + \epsilon_{13} \frac{\partial E_x}{\partial t} + \epsilon_{33} \frac{\partial E_z}{\partial t}. \quad (24)$$

These anisotropic equations generalize the isotropic model used by Greenfield and Wu [1]. On the other hand, in acoustics, uniform properties in the  $y$  direction imply that one of the shear waves has its own (decoupled) differential equation, known in the literature as the SH wave equation (e.g., Ref. [11]). This is strictly true in the plane of mirror symmetry of a monoclinic medium. Propagation in this plane implies pure anti-plane strain motion, and is the most general situation for which pure shear waves exist at all propagation angles. On the other hand, pure shear wave propagation in hexagonal media are a degenerate case. A set of parallel fractures embedded in a transversely isotropic formation can be represented by a monoclinic

medium. When the plane of mirror symmetry of this medium is vertical, the pure anti-plane strain waves are SH waves. Moreover, monoclinic media include many other cases of higher symmetry. Weak tetragonal media, strong trigonal media and orthorhombic media are subsets of the set of monoclinic media.

In a monoclinic medium, the elasticity and viscosity matrices and their inverses have the following form [8]

$$\begin{bmatrix} a_{11} & a_{12} & a_{13} & 0 & a_{15} & 0 \\ a_{12} & a_{22} & a_{23} & 0 & a_{25} & 0 \\ a_{13} & a_{23} & a_{33} & 0 & a_{35} & 0 \\ 0 & 0 & 0 & a_{44} & 0 & a_{46} \\ a_{15} & a_{25} & a_{35} & 0 & a_{55} & 0 \\ 0 & 0 & 0 & a_{46} & 0 & a_{66} \end{bmatrix}. \quad (25)$$

It is assumed that any kind of symmetry possessed by the attenuation follows the symmetry of the crystallographic form of the material. This statement can be supported by an empirical law known as Neumann's principle [12].

The relevant components describing the motion of the SH wave are

$$\begin{bmatrix} a_{44} & a_{46} \\ a_{46} & a_{66} \end{bmatrix}. \quad (26)$$

Then, the differential equations are obtained from the second row of (8) and the fourth and sixth rows of (19):

$$\frac{\partial \sigma_{xy}}{\partial x} + \frac{\partial \sigma_{yz}}{\partial z} = \rho \frac{\partial v_y}{\partial t} - F_y, \quad (27)$$

$$-\frac{\partial v_y}{\partial z} = -\tau_{44} \sigma_{yz} - \tau_{46} \sigma_{xy} - s_{44} \frac{\partial \sigma_{yz}}{\partial t} - s_{46} \frac{\partial \sigma_{xy}}{\partial t}, \quad (28)$$

$$\frac{\partial v_y}{\partial x} = \tau_{46} \sigma_{yz} + \tau_{66} \sigma_{xy} + s_{46} \frac{\partial \sigma_{yz}}{\partial t} + s_{66} \frac{\partial \sigma_{xy}}{\partial t}, \quad (29)$$

where

$$\begin{aligned} \tau_{44} &= \eta_{66}/\bar{\eta}, & \tau_{66} &= \eta_{44}/\bar{\eta}, & \tau_{46} &= -\eta_{46}/\bar{\eta}, \\ \bar{\eta} &= \eta_{44}\eta_{66} - \eta_{46}^2, \end{aligned} \quad (30)$$

and

$$s_{44} = c_{66}/c, \quad s_{66} = c_{44}/c, \quad s_{46} = -c_{46}/c, \\ c = c_{44}c_{66} - c_{46}^2, \quad (31)$$

where the stiffnesses  $c_{IJ}$  and the viscosities  $\eta_{IJ}$ , ( $I, J = 4, 6$ ) are the  $(I, J)$ -components of the matrices  $\mathbf{c}_M$  and  $\boldsymbol{\eta}_M$ , respectively.

Note that Eqs. (22)–(24) are converted into Eqs. (27)–(29), and vice versa, under the following substitutions:

$$\mathbf{V} \equiv \begin{bmatrix} v_y \\ \sigma_{yz} \\ \sigma_{xy} \end{bmatrix} \Leftrightarrow \begin{bmatrix} H_y \\ -E_x \\ E_z \end{bmatrix}, \quad (32)$$

$$F_y \Leftrightarrow M_y, \quad (33)$$

$$\mathbf{s} \equiv \begin{bmatrix} s_{44} & s_{46} \\ s_{46} & s_{66} \end{bmatrix} \Leftrightarrow \begin{bmatrix} \epsilon_{11} & -\epsilon_{13} \\ -\epsilon_{13} & \epsilon_{33} \end{bmatrix} \equiv \boldsymbol{\epsilon}', \quad (34)$$

$$\boldsymbol{\tau} \equiv \begin{bmatrix} \tau_{44} & \tau_{46} \\ \tau_{46} & \tau_{66} \end{bmatrix} \Leftrightarrow \begin{bmatrix} \sigma_{11} & -\sigma_{13} \\ -\sigma_{13} & \sigma_{33} \end{bmatrix} \equiv \boldsymbol{\sigma}', \quad (35)$$

$$\rho \Leftrightarrow \mu, \quad (36)$$

where  $\mathbf{s}$  and  $\boldsymbol{\tau}$  are redefined here as  $2 \times 2$  matrices for simplicity. Introducing the  $2 \times 2$  stiffness and viscosity matrices

$$\mathbf{c} = \begin{bmatrix} c_{44} & c_{46} \\ c_{46} & c_{66} \end{bmatrix}, \quad \boldsymbol{\eta} = \begin{bmatrix} \eta_{44} & \eta_{46} \\ \eta_{46} & \eta_{66} \end{bmatrix}, \quad (37)$$

we can get the 2D identities  $\mathbf{s} = \mathbf{c}^{-1}$  and  $\boldsymbol{\tau} = \boldsymbol{\eta}^{-1}$ , which are similar to the 3D equations (17) and (18), respectively. Then, the anisotropic SH wave equation based on a Maxwell rheology is mathematically equivalent to the anisotropic Maxwell equations whose forcing term is a magnetic current.

To get a more intuitive idea of our field equations, and to introduce the concept of quality factor, we develop the following considerations, which lead to Figures 1 and 2. It is well known that the mechanical representation of the Maxwell rheological model is a series connection of a spring and a dashpot. For instance, Eq. (29) with  $c_{46} = \eta_{46} = 0$  can be constructed from the model displayed in Figure 1, where  $\gamma_1$  and  $\gamma_2$  are the strains on the dashpot and on the spring, respectively. In fact,

$$\sigma_{xy} = \eta_{44} \frac{\partial \gamma_1}{\partial t} \quad \text{and} \quad \sigma_{xy} = c_{44} \gamma_2,$$

and

$$\frac{\partial}{\partial t}(\gamma_1 + \gamma_2) = \frac{\partial v_y}{\partial x},$$

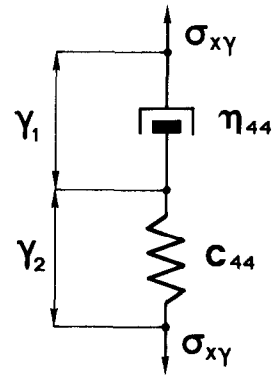


Fig. 1. Maxwell viscoelastic model corresponding to the  $xy$  component of the stress–strain constitutive relation, with  $c_{46} = \eta_{46} = 0$ . The strains acting on the dashpot and spring are  $\gamma_1$  and  $\gamma_2$ , respectively.

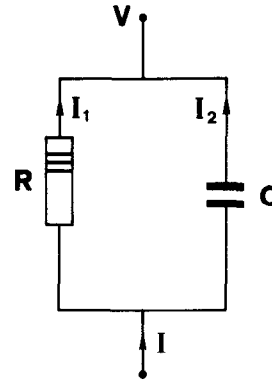


Fig. 2. Electric circuit equivalent to the viscoelastic model shown in Figure 1, where  $R$  and  $C$  are the resistance and capacitance,  $V$  is the voltage, and  $I_1$  and  $I_2$  are the electric currents. The analogy implies that the energy dissipated in the resistor is equivalent to the loss energy in the dashpot, and the energy stored in the capacitor is equivalent to the potential energy stored in the spring. On the other hand, the magnetic energy is equivalent to the elastic kinetic energy.

imply (29); indeed, if  $c_{46} = \eta_{46} = 0$ , then  $s_{44} = 1/c_{44}$  and  $\tau_{44} = 1/\eta_{44}$ .

Obtaining a pictorial representation of the electromagnetic field equations is not so easy. However, if, instead of the distributed-parameter system (23) and (24), we consider the corresponding lumped-parameter system (electric circuit), then such an interpretation becomes straightforward. Indeed, if we consider, for example, Eq. (23) and assume, for simplicity, that  $\sigma_{13} = \epsilon_{13} = 0$ , then its r.h.s. becomes

$$\sigma_{11} E_x + \epsilon_{11} \frac{\partial E_x}{\partial t}$$

or, in terms of circuit elements,

$$\frac{1}{R} V + C \frac{dV}{dt} \equiv I_1 + I_2 \equiv I,$$

which corresponds to a parallel connection of a capacitor and a resistor as shown in Figure 2, where  $R$  and  $C$  are the resistance and the capacitance, respectively,  $V$  is the voltage (i.e., the integral of the electric field) and  $I_1$  and  $I_2$  are the electric currents ( $V/R$  corresponds to  $\sigma E$ ). At first sight it is surprising that a series circuit, as in Figure 1, may be the analogue of a parallel circuit, as in Figure 2; but this is the outcome of the mathematical machinery embodied in the field equations and in the correspondence (32)–(36). An important parameter of the circuit represented in Figure 2 is the loss tangent of the capacitor. The circuit can be considered as a real capacitor whose losses are modeled by the resistor  $R$ . Under the action of a harmonic voltage of frequency  $\omega$ , the total current  $I$  is not in quadrature with the voltage, but makes an angle  $\pi/2 - \delta$  with it ( $I_1$  is in phase with  $V$ , while  $I_2$  is in quadrature). As a consequence, the loss tangent is given by

$$\tan \delta = \frac{I_1}{I_2} = \frac{I \cos(\pi/2 - \delta)}{I \sin(\pi/2 - \delta)}. \quad (38)$$

Multiplying and dividing (38) by  $V$  gives the relation between the dissipated power in the resistor and the reactive power in the capacitor

$$\tan \delta = \frac{VI \cos(\pi/2 - \delta)}{VI \sin(\pi/2 - \delta)} = \frac{V^2/R}{\omega CV^2} = \frac{1}{\omega CR}. \quad (39)$$

The quality factor of the circuit is the inverse of the loss tangent. In terms of permittivity and conductivity it is given by

$$Q = \frac{\epsilon}{\sigma}. \quad (40)$$

At the end of the next section, the preceding formula for the quality factor will be obtained from the acoustic–electromagnetic analogy.

## 5. Kinematics and energy considerations

The kinematic quantities describing wave motion are the slowness, the phase velocity and the attenua-

tion vectors. The analysis is carried out for the acoustic case, and the electromagnetic case is obtained by applying equivalence (32)–(36). For a harmonic plane wave of angular frequency  $\omega$ , Cauchy's equation (8) – in absence of body forces – becomes

$$\nabla \cdot \mathbf{T} - i\omega \rho \mathbf{v} = 0. \quad (41)$$

On the other hand, the generalized Maxwell stress–strain relation (15) takes the form

$$\mathbf{T} = \mathbf{p} \cdot \mathbf{S}, \quad (42)$$

where  $\mathbf{p}$  is the complex stiffness matrix given by

$$\mathbf{p} = \left( \mathbf{s} - \frac{i}{\omega} \boldsymbol{\tau} \right)^{-1}. \quad (43)$$

All the matrices in this equation have dimension six. However, since the SH mode is pure, a similar equation can be obtained for matrices of the form (21). In this case, the stress and strain simplify to

$$\mathbf{T} = [\sigma_{yz}, \sigma_{xy}]^T \quad \text{and} \quad \mathbf{S} = \left[ \frac{\partial u_y}{\partial z}, \frac{\partial u_y}{\partial x} \right]^T, \quad (44)$$

respectively, where  $u_y$  is the displacement field.

The displacement associated to a homogeneous viscoelastic SH plane wave has the form

$$\mathbf{u} = u_y \mathbf{e}_2, \quad u_y = U_0 e^{i(\omega t - \mathbf{k} \cdot \mathbf{x})}, \quad \mathbf{e}_2 = [0, 1, 0]^T, \quad (45)$$

where  $\mathbf{x} = (x, z)$  is the position vector and

$$\mathbf{k} = (\kappa - i\alpha) \hat{\mathbf{k}} = k \hat{\mathbf{k}} \quad (46)$$

is the complex wavevector, with

$$\hat{\mathbf{k}} = [l_x, l_z]^T \quad (47)$$

defining the propagation direction through the direction cosines  $l_x$  and  $l_z$ . Replacing the stress–strain Eq. (42) into Cauchy's equations (41) yields the dispersion relation

$$p_{66} l_x^2 + 2p_{46} l_x l_z + p_{44} l_z^2 - \rho \left( \frac{\omega}{k} \right)^2 = 0. \quad (48)$$

This relation defines the complex velocity

$$V \equiv \frac{\omega}{k} = \left( \frac{p_{66} l_x^2 + 2p_{46} l_x l_z + p_{44} l_z^2}{\rho} \right)^{1/2}. \quad (49)$$

The real slowness and attenuation vectors can be expressed in terms of the complex velocity as

$$\mathbf{s} = \Re\left(\frac{1}{V}\right) \hat{\mathbf{k}}, \quad (50)$$

and

$$\boldsymbol{\alpha} = -\omega \Im\left(\frac{1}{V}\right) \hat{\mathbf{k}}, \quad (51)$$

while the phase velocity is the reciprocal of the slowness. In vector form it is given by

$$\mathbf{V}_p = \left[ \Re\left(\frac{1}{V}\right) \right]^{-1} \hat{\mathbf{k}}. \quad (52)$$

The operators  $\Re(\cdot)$  and  $\Im(\cdot)$  take the real and imaginary part, respectively. The velocity of the energy (wavefront) is defined as the average power flow density divided by the average energy density. The power flow is the real part of the Umov–Poynting vector, while the average energy is half the sum of the peak kinetic and potential energy densities (see Ref. [13]). The calculation of these quantities is carried out in Appendix B. Hence, the energy velocity is

$$\mathbf{V}_e = \frac{V_p}{\Re(V)} \left\{ \Re\left(\frac{1}{\rho V}\right) [(p_{66}l_x + p_{46}l_z)\hat{\mathbf{e}}_1 + (p_{44}l_z + p_{46}l_x)\hat{\mathbf{e}}_3] \right\}, \quad (53)$$

where  $\hat{\mathbf{e}}_1$  and  $\hat{\mathbf{e}}_3$  are the unit vectors along the  $x$  and  $z$  directions, respectively. As shown in Appendix B, the quality factor is given by

$$Q = \frac{\Re(V^2)}{\Im(V^2)}. \quad (54)$$

From Eq. (43), in virtue of the acoustic–electromagnetic correspondence (32)–(36), it follows that  $\mathbf{p}$  corresponds to the inverse of the complex permittivity matrix  $\boldsymbol{\epsilon}^*$ , namely:

$$\mathbf{p}^{-1} \Leftrightarrow \boldsymbol{\epsilon}^* = \boldsymbol{\epsilon}' - \frac{i}{\omega} \boldsymbol{\sigma}'. \quad (55)$$

Then, the electromagnetic slowness, attenuation, phase and energy velocities, and quality factor can be calculated from equations (50), (51), (52), (53) and (54) by applying this equivalence, and that of the density with the permeability (36), to Eq. (49).

In orthorhombic media, the components of the form  $a_{46}$  vanish; therefore the complex stiffness matrix is diagonal, with components

$$(c_{II}^{-1} - i\omega^{-1}\eta_{II}^{-1})^{-1} \quad (56)$$

in the acoustic case, where  $I = 4$  or  $6$ , and

$$(\epsilon_{II} - i\omega^{-1}\sigma_{II})^{-1} \quad (57)$$

in the electromagnetic case, where  $I = 1$  or  $3$ . In isotropic media, where  $a_{44} = a_{66}$ , the complex velocity becomes

$$V = [(G^{-1} - i\omega^{-1}\eta^{-1})\rho]^{-1/2} \quad (58)$$

in the acoustic case, and

$$V = [(\epsilon - i\omega^{-1}\sigma)\mu]^{-1/2}, \quad (59)$$

in the electromagnetic case, where  $G$  is the rigidity modulus,  $\eta$  is the viscosity,  $\epsilon$  is the permittivity, and  $\sigma$  is the conductivity.

It is clear that the kinetic and strain energy densities are associated with the magnetic and electric energy densities. In terms of circuit elements, the kinetic, strain and dissipated energies represent the energies stored in inductances, capacitors and the dissipative ohmic losses, respectively. A similar analogy, used by Maxwell, can be established between particle mechanics and circuits (e.g., Ref. [14]).

In the isotropic case, the acoustic and electromagnetic quality factors are

$$Q_{ac} = \omega \frac{\eta}{G}, \quad (60)$$

and

$$Q_{em} = \omega \frac{\epsilon}{\sigma}. \quad (61)$$

respectively. If  $\eta \rightarrow 0$  and  $\sigma \rightarrow \infty$ , then the behaviour is diffusive; while conditions  $\eta \rightarrow \infty$  and  $\sigma \rightarrow 0$  correspond to the elastic limit. Note that  $\eta/G$  and  $\epsilon/\sigma$  are the relaxation times of the wave processes.

## 6. Wave equation and simulations

Equations (28) and (29) can be written in compact form as

$$\mathbf{s} \cdot \frac{\partial \mathbf{T}}{\partial t} = \nabla_2 v_y - \boldsymbol{\tau} \cdot \mathbf{T}, \quad (62)$$

which can be also deduced from (19) by using the 2D notation, with  $\nabla_2 = [\partial/\partial z, \partial/\partial x]^T$ . Multiplying (62) by  $\mathbf{c}$  gives

$$\frac{\partial \mathbf{T}}{\partial t} = \mathbf{c} \cdot (\nabla_2 v_y - \boldsymbol{\tau} \cdot \mathbf{T}). \quad (63)$$

Cauchy's equation (27) becomes

$$\frac{\partial v_y}{\partial t} = \frac{1}{\rho} (\nabla_2^T \cdot \mathbf{T} - F_y). \quad (64)$$

Equations (63) and (64) represent the velocity–stress formulation of the problem for the unknown vector  $\mathbf{V}$  defined in (32). The wave equation has the form

$$\frac{\partial \mathbf{V}}{\partial t} = \mathbf{M} \mathbf{V} + \mathbf{F}', \quad (65)$$

where  $\mathbf{M}$  is a spatial differential operator matrix. Most frequently, an explicit or implicit finite-difference scheme is used to march the solution in time. This technique is based on a Taylor expansion of the evolution operator. Here, Eq. (65) is solved by a spectral time integration technique introduced in Ref. [15]. Its formal solution is

$$\mathbf{V}(t) = \int_0^t e^{\theta \mathbf{M}} \mathbf{F}'(t - \theta) d\theta, \quad (66)$$

where zero initial conditions have been assumed. In Eq. (66),  $\exp(\theta \mathbf{M})$  is called the evolution operator of the system. The corresponding numerical algorithm is based on a polynomial interpolation of the exponential function in the complex domain of the eigenvalues of the operator  $\mathbf{M}$ , over a set of points which is known to have some optimal interpolation properties. These points should lie on a T-shape domain defined by the imaginary axis and the negative real semiaxis of the complex frequency plane. In this way, the interpolating polynomial is “almost best”. In the isotropic case, the eigenvalues  $\lambda = i\omega$  ( $\omega$  complex) of  $\mathbf{M}$  satisfy the following characteristic equation:

$$\left(\lambda + \frac{\eta}{G}\right) \left[\lambda \left(\lambda + \frac{\eta}{G}\right) + \frac{G}{\rho} \kappa^2\right] = 0, \quad (67)$$

where  $\kappa$  is the real wavenumber. The solution of (67) gives a static mode corresponding to the eigenvalue  $\lambda = -\eta/G$ , and two propagating modes lying close to the imaginary axis, corresponding to the other eigenvalues. Note that  $\eta/G$  is the relaxation time of the

Table 1  
Material properties

|  |   |
|--|---|
| Elasticities (GPa)   | $c_{44} = 10.0, c_{66} = 22.5, c_{46} = -5.0$   |
| Viscosities (GPa s)  | $\eta_{44} = 1.50, \eta_{66} = 3.40, \eta_{46} = 1.13$  |
| Permittivities   | $\epsilon_{11} = 12.5\epsilon_0, \epsilon_{33} = 17.5\epsilon_0,$<br>$\epsilon_{13} = -4.3\epsilon_0$         |
| Conductivities (S m <sup>-1</sup> )  | $\sigma_{11} = 3.0 \times 10^{-5}, \sigma_{33} = 7.0 \times 10^{-5},$<br>$\sigma_{13} = -3.46 \times 10^{-5}$ |
| <hr/>  |   |
| $\epsilon_0 = 8.85 \times 10^{-12}$ F m <sup>-1</sup> ; $\mu = \mu_0 = 4\pi \times 10^{-7}$ H m <sup>-1</sup> ;<br>$\rho = 2.5$ g cm <sup>-3</sup> |   |
| <hr/>  |   |

system, and  $G/\rho$  is the square of the phase velocity at high frequencies. It can be seen that, also in the anisotropic case, the eigenvalues lie on the T-shape domain.

To balance time integration and spatial accuracies, the spatial derivatives are computed by means of the Fourier pseudospectral method, although finite-differences or finite-elements can also be used.

The material properties of the medium are given in Table 1, where  $\epsilon_0$  and  $\mu_0$  are the permittivity and permeability of free space. Fig. 3 shows slowness (a), attenuation (b), energy velocity (c) and quality factor (d) surfaces for homogeneous electromagnetic plane waves at a frequency of 600 kHz. The orientation and shape of the curves depend on the dielectric and conductivity tensors. As can be seen, the attenuation is highly anisotropic, with maximum dissipation at approximately 30 degrees from the horizontal axis. Analogously, the slowness has an anisotropic character, while the energy velocity indicates the shape of the wavefront.

The rectangular numerical mesh has  $N_x = N_z = 105$  grid points per side, with a uniform grid spacing of  $D_x = D_z = 30$  m in the electromagnetic simulation, and  $D_x = D_z = 20$  m in the acoustic simulation. The field is initiated by a line source, normal to the  $(x, z)$ -plane. The source central frequency is 300 kHz and 50 Hz for the electromagnetic and acoustic cases, respectively. The cutoff frequency is twice the central frequency.

Fig. 4 compares numerical and analytical electromagnetic solutions of the magnetic field at a receiver whose location  $(x, z)$ , relative to the source, is indicated in the picture. The distance between the source and the receiver is 600 m. As can be appreciated, the agreement between solutions is virtually perfect de-

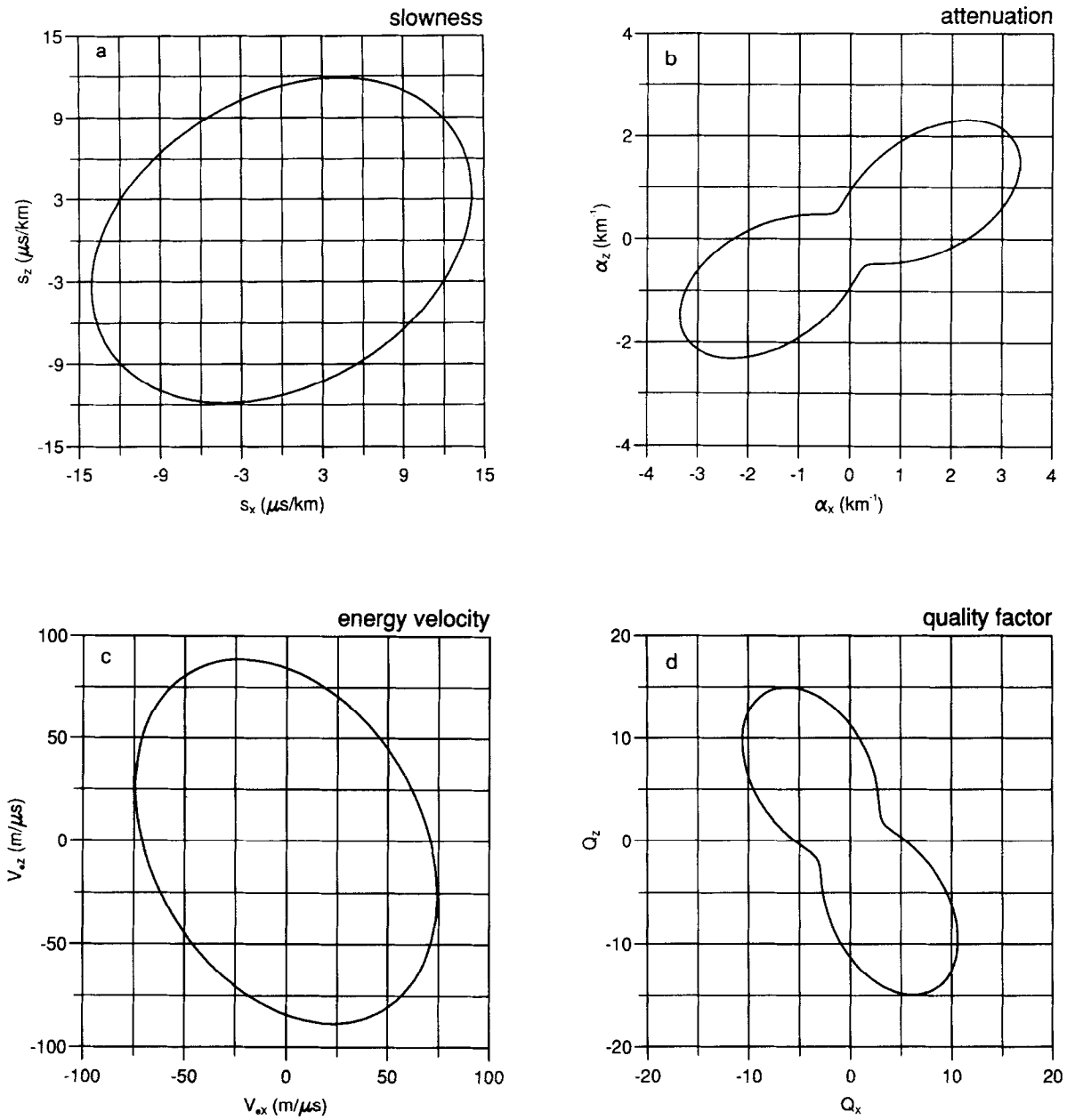


Fig. 3. Polar diagrams of the slowness (a), attenuation (b), energy velocity (c) and quality factor (d) curves for electromagnetic plane waves at a frequency of 600 kHz.

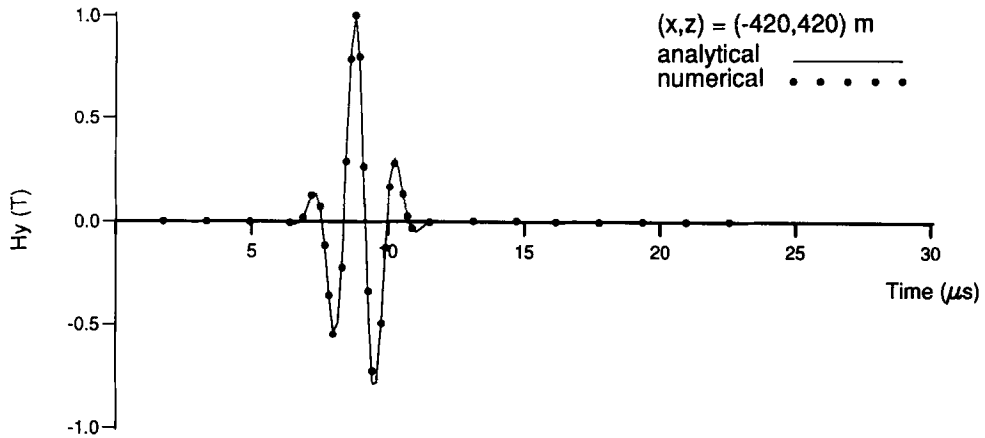


Fig. 4. Comparison between numerical and analytical electromagnetic solutions. The source central frequency is 300 kHz and the source–receiver distance is 600 m.

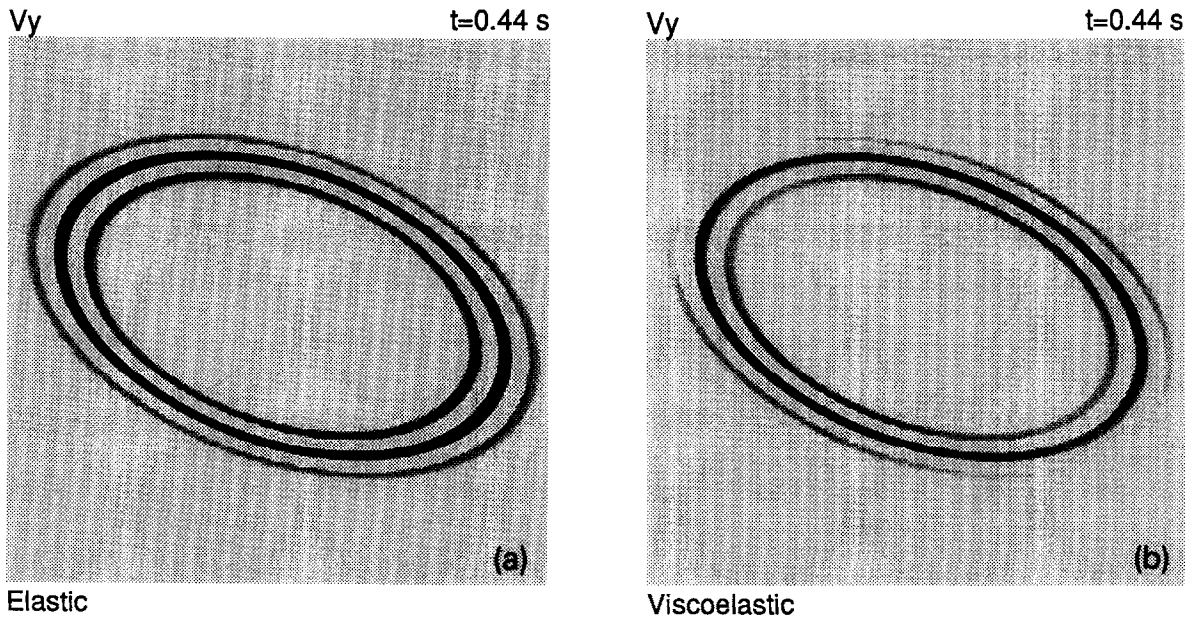


Fig. 5. Snapshots of the elastic (a) and viscoelastic (b) acoustic fields at 0.44 s. The elastic wavefront is slightly wider than the viscoelastic wavefront, since the phase velocity in a Maxwell material vanishes at zero frequency and approaches the elastic velocity at infinite frequency.

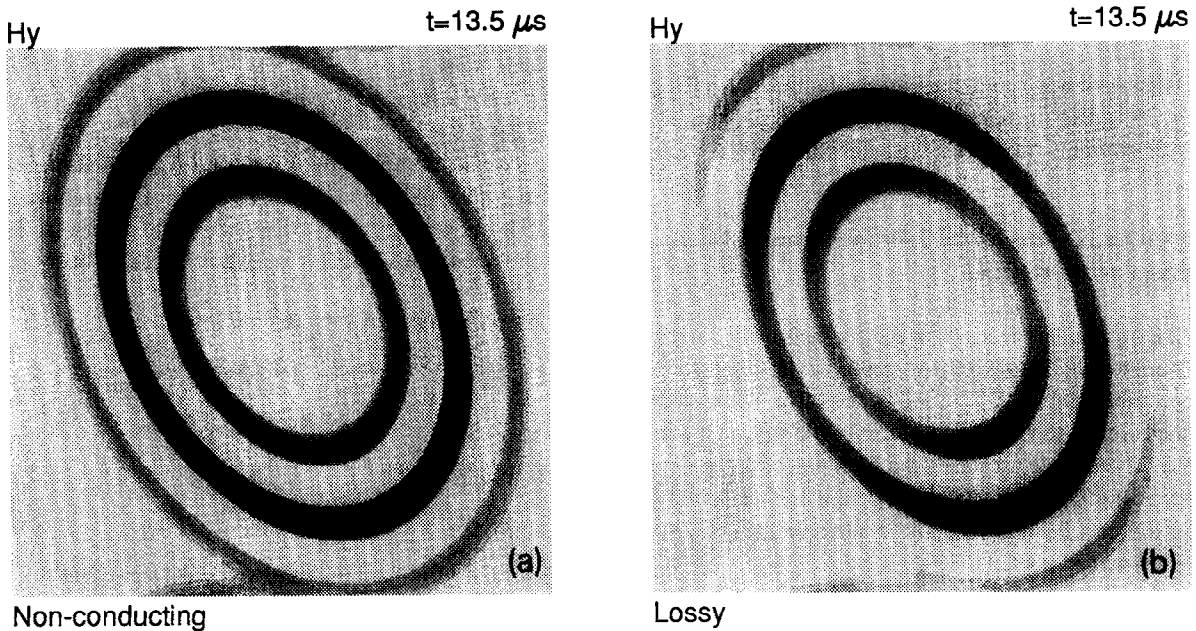


Fig. 6. Snapshots of the electromagnetic wavefield in the purely dielectric (a) and conducting (b) cases at  $13.5 \mu\text{s}$ . The anisotropic dissipation features are in agreement with the attenuation curve represented in Fig. 3b.

spite the anomalous behaviour of the phase velocity at low frequencies. Fig. 5 represents snapshots of the particle velocity  $v_y$  at  $t = 0.44 \text{ s}$ , where (a) corresponds to the elastic limit ( $\eta \rightarrow \infty$ ) and (b) is the viscoelastic case. Finally, Fig. 6 displays snapshots of the magnetic component  $H_y$  at  $t = 1.35 \mu\text{s}$ , where (a) corresponds to the elastic limit ( $\sigma \rightarrow 0$ ) and (b) is the dissipative case. The results given in Figs. 5 and 6 were obtained by using the same computer code with different input data. As can be seen, the snapshots of the lossy medium exhibit more anisotropic dissipation than in the lossless case. The features of the lossy electromagnetic snapshot are in agreement with the attenuation and energy velocity curves displayed in Fig. 3b and 3c, respectively.

This type of numerical modeling can be effectively used to simulate electromagnetic waves in heterogeneous media also [16].

## 7. Conclusions

We have exhibited an invertible correspondence between physical quantities that transform the SH (shear-horizontal) viscoelastic equations into the

TEM (transverse-electromagnetic) equations. The underlying assumptions are that the medium has monoclinic symmetry and, for simplicity, the electric source currents are zero. The analogy constitutes a mathematical equivalence that allows the acoustic and electromagnetic problems to be solved with the same analytical methodology. Therefore, the analysis of viscoelastic plane waves can be applied to the electromagnetic case. Similarly, the transient solution obtained in the viscoelastic case corresponds to the electromagnetic solution. In these cases, the equivalence is basically a correspondence between stiffness and permittivity, which are complex and frequency-dependent matrices. The most powerful application of the analogy is the use of the same computer code to solve acoustic and electromagnetic propagation problems in general inhomogeneous media. A challenging problem for future research is to generalize these results from two to three dimensions and/or to release the assumption on the material symmetry.

## Acknowledgments

This work was funded in part by the European Commission in the framework of the JOULE programme, subprogramme Advanced Fuel Technologies.

## Appendix A. Analytical solution in unbounded homogeneous media

The analytical solution for the anelastic problem can be obtained by means of the correspondence principle (e.g., Ref. [9]). This requires to know the explicit expression of the elastic solution in the frequency domain. Then, the elasticities can be replaced by the corresponding complex stiffnesses, and the viscoelastic solution can be obtained by an inverse time Fourier transform.

Considering the elastic case in (62), i.e.  $\tau = 0$ , and eliminating the stress tensor by using (64) gives

$$(\nabla_2^T \cdot \mathbf{c} \cdot \nabla_2) v_y - \rho \ddot{v}_y = \dot{F}_y, \quad (\text{A.1})$$

where the dot above a variable denotes time differentiation. Since we consider here a homogeneous medium, Eq. (A.1) becomes

$$\left( c_{44} \frac{\partial^2}{\partial z^2} + c_{66} \frac{\partial^2}{\partial x^2} + 2c_{46} \frac{\partial^2}{\partial x \partial z} \right) v_y - \rho \ddot{v}_y = \dot{F}_y. \quad (\text{A.2})$$

We show below that it is possible, by a transformation of coordinates, to transform the spatial differential operator on the r.h.s. of (A.2) to a pure Laplacian differential operator. In that case, Eq. (A.2) becomes

$$\left( \frac{\partial^2}{\partial z'^2} + \frac{\partial^2}{\partial x'^2} \right) v_y - \rho \ddot{v}_y = \dot{F}_y. \quad (\text{A.3})$$

Considering the solution for the Green's function (i.e., the r.h.s. of (A.3) is a localized delta function in time and space at the origin), and transforming the wave equation to the frequency domain, gives

$$\left( \frac{\partial^2}{\partial z'^2} + \frac{\partial^2}{\partial x'^2} \right) \tilde{g} + \rho \omega^2 \tilde{g} = -4\pi \delta(x') \delta(z'), \quad (\text{A.4})$$

where  $\tilde{g}$  is the Fourier transform of the Green's function. The constant  $-4\pi$  is introduced for convenience. The solution of (A.4) is (e.g., Ref. [17])

$$\tilde{g}(x', z', \omega) = -i\pi H_0^{(2)}(\sqrt{\rho\omega} r'), \quad (\text{A.5})$$

where  $H_0^{(2)}$  is the Hankel function of the second kind, and

$$r' = (x'^2 + z'^2)^{1/2} \equiv (\mathbf{x}'^T \cdot \mathbf{x}')^{1/2}. \quad (\text{A.6})$$

We have to compute the r.h.s. of (A.5) in terms of the original position vector  $\mathbf{x} = [z, x]^T$ . Diagonalizing matrix  $\mathbf{c}$  as  $\mathbf{c} = \mathbf{A} \cdot \mathbf{\Lambda} \cdot \mathbf{A}^T$ , where  $\mathbf{\Lambda}$  is the matrix of the eigenvalues, the Laplacian operator in (A.1) becomes

$$\begin{aligned} \nabla_2^T \cdot \mathbf{c} \cdot \nabla_2 &= \nabla_2^T \cdot \mathbf{A} \cdot \mathbf{\Lambda} \cdot \mathbf{A}^T \cdot \nabla_2 \\ &= \nabla_2^T \cdot \mathbf{A} \cdot \mathbf{\Omega} \cdot \mathbf{\Omega} \cdot \mathbf{A}^T \cdot \nabla_2 \\ &= \nabla_2'^T \cdot \nabla_2', \end{aligned} \quad (\text{A.7})$$

where  $\mathbf{\Lambda} = \mathbf{\Omega}^2$ , and

$$\nabla_2' = \mathbf{\Omega} \cdot \mathbf{A}^T \cdot \nabla_2. \quad (\text{A.8})$$

Using that  $\mathbf{\Omega}$  is diagonal and  $\mathbf{A}^T = \mathbf{A}^{-1}$ , we get

$$\mathbf{x}' = \mathbf{\Omega}^{-1} \cdot \mathbf{A}^T \cdot \mathbf{x}. \quad (\text{A.9})$$

Substituting (A.9) into Eq. (A.6) gives

$$\begin{aligned} \mathbf{x}'^T \cdot \mathbf{x}' &= \mathbf{x}^T \cdot \mathbf{A} \cdot \mathbf{\Omega}^{-1} \cdot \mathbf{\Omega}^{-1} \cdot \mathbf{A}^T \cdot \mathbf{x} \\ &= \mathbf{x}^T \cdot \mathbf{A} \cdot \mathbf{\Lambda}^{-1} \cdot \mathbf{A}^T \cdot \mathbf{x}. \end{aligned} \quad (\text{A.10})$$

But, since  $\mathbf{A} \cdot \mathbf{\Lambda}^{-1} \cdot \mathbf{A}^T = \mathbf{c}^{-1}$ , we finally have

$$\begin{aligned} r'^2 &= \mathbf{x}^T \cdot \mathbf{c}^{-1} \cdot \mathbf{x} \\ &= (c_{66}z^2 + c_{44}x^2 - 2c_{46}xz)/c, \end{aligned} \quad (\text{A.11})$$

where  $c$  is the determinant of  $\mathbf{c}$  given by Eq. (31).

Application of the correspondence principle to the elastic Green's function

$$\tilde{g}(x, z, \omega) = -i\pi H_0^{(2)}[\omega(\mathbf{x}^T \cdot \rho \mathbf{c}^{-1} \cdot \mathbf{x})^{1/2}], \quad (\text{A.12})$$

gives the viscoelastic Green's function

$$\tilde{g}_v(x, z, \omega) = -i\pi H_0^{(2)}[\omega(\mathbf{x}^T \cdot \rho \mathbf{p}^{-1} \cdot \mathbf{x})^{1/2}], \quad (\text{A.13})$$

where  $\mathbf{p}$  is given by (43). Note that in the electromagnetic case the solution is

$$\tilde{g}_{el}(x, z, \omega) = -i\pi H_0^{(2)}[\omega(\mathbf{x}^T \cdot \boldsymbol{\mu} \boldsymbol{\epsilon}^* \cdot \mathbf{x})^{1/2}], \quad (\text{A.14})$$

in virtue of the equivalence (32)–(36), and Eq. (55). When solving the wave propagation problem with numerical techniques, the Green function is multiplied with the Fourier transform of a band limited wavelet.

In this case, the transform of the source term in Eq. (A.2) is  $i\omega\tilde{F}_y$ . Therefore, the viscoelastic solution is

$$\tilde{v}_y(\mathbf{x}, \omega) = \pi\omega\tilde{F}_y H_0^{(2)} \left[ \omega(\mathbf{x}^T \cdot \rho\mathbf{p}^{-1} \cdot \mathbf{x})^{1/2} \right], \quad (\text{A.15})$$

and the electromagnetic solution is

$$\tilde{H}_y(\mathbf{x}, \omega) = \pi\omega\tilde{M}_y H_0^{(2)} \left[ \omega(\mathbf{x}^T \cdot \mu\boldsymbol{\epsilon}^* \cdot \mathbf{x})^{1/2} \right], \quad (\text{A.16})$$

To ensure a time-domain real solution we take, for  $\omega < 0$ ,

$$\tilde{v}_y(\mathbf{x}, \omega) = \bar{\tilde{v}}_y(\mathbf{x}, -\omega), \quad (\text{A.17})$$

where the bar denotes complex conjugation. Finally, the time domain solution is obtained by an inverse transform based on the Fast Fourier Transform.

### Appendix B. Umov–Poynting vector, energy densities, and quality factor for SH waves in monoclinic viscoelastic media

By Eq. (45), the nonzero strain components are

$$S_4 = \frac{\partial u_y}{\partial z} = -ikl_z u_y \quad \text{and} \quad S_6 = \frac{\partial u_y}{\partial x} = -ikl_x u_y. \quad (\text{B.1})$$

Hence, the nonzero stress components are

$$T_4 = p_{44}S_4 + p_{46}S_6 = -iku_y(p_{44}l_z + p_{46}l_x) \quad (\text{B.2})$$

and

$$T_6 = p_{66}S_6 + p_{46}S_4 = -iku_y(p_{66}l_x + p_{46}l_z). \quad (\text{B.3})$$

The Umov–Poynting vector is [13]

$$\mathbf{P} = -\frac{1}{2}\boldsymbol{\Sigma} \cdot \mathbf{v}^*, \quad (\text{B.4})$$

where

$$\boldsymbol{\Sigma} = \begin{bmatrix} T_1 & T_6 & T_5 \\ T_6 & T_2 & T_4 \\ T_5 & T_4 & T_3 \end{bmatrix} \quad (\text{B.5})$$

and therefore, in the monoclinic case,

$$\begin{aligned} \mathbf{P} &= -\frac{1}{2}\dot{u}^* \mathbf{T} [T_6, 0, T_4]^T \\ &= \frac{\omega^2}{2V}|U_0|^2 e^{-i\omega t} e^{-2\alpha\boldsymbol{\kappa} \cdot \mathbf{x}} \begin{bmatrix} p_{46}l_z + p_{66}l_x \\ 0 \\ p_{44}l_z + p_{46}l_x \end{bmatrix}. \quad (\text{B.6}) \end{aligned}$$

The peak kinetic energy density is [18]

$$(\epsilon_v)_{\text{peak}} = \frac{1}{2}\rho\mathbf{v}^* \cdot \mathbf{v} = \frac{1}{2}\rho\omega^2|U_0|^2 e^{-2\alpha\boldsymbol{\kappa} \cdot \mathbf{x}}. \quad (\text{B.7})$$

Likewise, the peak potential energy density is

$$\begin{aligned} (\epsilon_s)_{\text{peak}} &= \frac{1}{2}\Re(p_{44}|S_4|^2 + p_{66}|S_6|^2 \\ &\quad + p_{46}(S_4S_6^* + S_4^*S_6)) \\ &= \frac{1}{2}\rho\omega^2|U_0|^2 e^{-2\alpha\boldsymbol{\kappa} \cdot \mathbf{x}} \frac{\Re(V^2)}{|V|^2} \end{aligned} \quad (\text{B.8})$$

and the average dissipated energy density is

$$(\epsilon_d)_{AV} = \frac{1}{2}\rho\omega^2|U_0|^2 e^{-2\alpha\boldsymbol{\kappa} \cdot \mathbf{x}} \frac{\Im(V^2)}{|V|^2}. \quad (\text{B.9})$$

Finally, using the last two equations, we get the quality factor

$$Q = \frac{(\epsilon_s)_{\text{peak}}}{(\epsilon_d)_{AV}} = \frac{\Re(V^2)}{\Im(V^2)}. \quad (\text{B.10})$$

### References

- [1] R. J. Greenfield, and T. Wu, Electromagnetic wave propagation in disrupted coal seams, *Geophysics* 56, 1571–1577 (1991).
- [2] C. W. F. Everitt, 1975, *James Clerk Maxwell, Physicist and Natural Philosopher*, Charles Scribner's Sons (1975).
- [3] J. Hendry, *James Clerk Maxwell and the Theory of the Electromagnetic Field*, Adam Hilger Ltd, Bristol and Boston (1986).
- [4] J. C. Maxwell, On the dynamical theory of gases, *Phil. Trans. R. Soc.* 157, 49–88 (1867).
- [5] J. C. Maxwell, *The Scientific Papers of James Clerk Maxwell*, ed. W. D. Niven, 2 volumes, Cambridge University Press, Cambridge (1890).
- [6] D. R. Bland, *Wave theory and applications*, Clarendon Press, Oxford (1988).
- [7] W. C. Chew, *Waves and fields in inhomogeneous media*, Van Nostrand Reinhold, New York (1990).
- [8] B. A. Auld, *Acoustic fields and waves in solids, Vol. 1*, Robert E. Krieger, Publishing Co., Malabar, Florida (1990).
- [9] A. Ben-Menahem and S. G. Singh, *Seismic waves and sources*, Springer Verlag, New York (1981).
- [10] G. Casula and J. M. Carcione, Generalized mechanical model analogies of linear viscoelastic behaviour, *Boll. Geofis. Teor. Appl.* 34, 235–256 (1992).
- [11] J. Virieux, SH-wave propagation in heterogeneous media: Velocity–stress finite-difference method, *Geophysics* 49, 1933–1957 (1984).
- [12] F. E. Neumann, *Vorlesungen über die Theorie der Elasticität*, Leipzig (1885).

- [13] J. M. Carcione and F. Cavallini, Energy balance and fundamental relations in anisotropic viscoelastic media, *Wave Motion* 18, 11–20 (1993).
- [14] P. Hammond, *Energy methods in electromagnetism*, Clarendon Press, Oxford (1981).
- [15] H. Tal-Ezer, J. M. Carcione, and D. Kosloff, An accurate and efficient scheme for wave propagation in linear viscoelastic media, *Geophysics* 55, 1366–1379 (1990).
- [16] J. M. Carcione and F. Cavallini, Modeling transverse electromagnetic waves in conducting anisotropic media by a spectral time-domain technique, in A. Terzuoli, Ed., 10th Annual Review of Progress in Applied Computational Electromagnetics, Vol. II, 586–593, Monterey CA (1994).
- [17] P. M. Morse and H. Feshbach, *Methods of theoretical physics*, McGraw-Hill, New-York (1953).
- [18] J. M. Carcione, Wavefronts in dissipative anisotropic media, *Geophysics* 59, 644–657 (1994).